



Enhanced photocatalytic activity of C–N–S-tridoped TiO₂ towards degradation of methyl orange and phenol

Jiufu Chen^a, Junbo Zhong^{a,*}, Jianzhang Li^a, Shengtian Huang^a, Minjiao Li^{a,b}

^aKey Laboratory of Green Catalysis of Higher Education Institutes of Sichuan, College of Chemistry and Environmental Engineering, Sichuan University of Science and Engineering, Zigong 643000, China, emails: junbozhong@163.com (J. Zhong), cjf2171@163.com (J. Chen), lyl63@sina.com (J. Li), sth499@163.com (S. Huang), lmj0621@126.com (M. Li)

^bSichuan Provincial Academician (Expert) Workstation, Sichuan University of Science and Engineering, Zigong 643000, China

Received 18 March 2016; Accepted 15 October 2016

ABSTRACT

In this paper, C–N–S-tridoped TiO₂ was successfully prepared through a sol–gel routine using ammonium thiocyanate as dopant after annealing at 823 K and characterized by Brunauer–Emmett–Teller method, X-ray diffraction, UV/Vis diffuse reflectance spectroscopy, scanning electron microscope, X-ray photoelectron spectroscopy and surface photovoltage spectroscopy. Doping C, N and S into the lattice of TiO₂ inhibits the growth of its crystal, changes the morphology and the surface hydroxyl content, widens the band gap and greatly enhances the photoinduced charge separation rate. The photocatalytic activities were evaluated by degradation of methyl orange and phenol aqueous solution. The results show that photocatalytic activity of the bare TiO₂ can be boosted by C–N–S tridoping.

Keywords: TiO₂; Tridoping; Photocatalytic activity; Charge separation; Degradation

1. Introduction

Semiconductor-based photocatalysis has aroused worldwide research interest owing to its potential applications in the decomposition of hazardous environmental contaminants [1,2]. Among the photocatalysts developed, TiO₂ is the most prospective photocatalyst due to its outstanding properties [3,4]. However, the photocatalytic activity of TiO₂ is far from efficient to meet the practical applications and limited by the high recombination of electron–hole, therefore, it is crucial to boost its photocatalytic efficiency. Tremendous efforts have been developed to promote the photocatalytic performance of TiO₂, among these approaches, doping with nonmetal elements is an effective and simple strategy [4,5].

To achieve nonmetal elements doping, different dopants were applied. Among all the dopants, ammonium thiocyanate has attracted increasing attention. Ammonium thiocyanate can be dissolved in ethanol and water, thus it is feasible

that C, N and S can be simultaneously doped into TiO₂ by a sol–gel routine using ammonium thiocyanate as dopant. However, the effects of the photoinduced charge separation rate and band gap on the photocatalytic activity of TiO₂ prepared by the sol–gel method using ammonium thiocyanate as dopant have been seldom addressed.

The objective of this paper is to investigate C–N–S tridoping on the band gap and the photoinduced charge separation rate and the relation with the photocatalytic activity. The photocatalytic performance was evaluated by degradation of methyl orange (MO) aqueous solution and phenol. In this paper, some novel results were obtained and discussed.

2. Experimental section

All chemicals (analytical grade reagents) were supplied from Chengdu Kelong Chemical Reagent Factory and used as received. Doped TiO₂ was prepared as the method described in reference [6] with some modification. Tetrabutyl orthotitanate (17 mL) and diethanolamine (5 mL) were dissolved

* Corresponding author.

in ethanol (67 mL), after vigorously stirring for 2 h at room temperature, forming A solution. Desired ammonium thiocyanate was dissolved in a mixed solution of water (3 mL) and ethanol (7 mL), resulting in B solution. The molar ratio of ammonium thiocyanate/Ti(OC₄H₉)₄ is 2%, 4%, 6%, 8% and 10%, respectively. The B solution was added dropwise to the A solution under stirring, resulting in a TiO₂ sol. The dried gel was annealed at 823 K for 1 h in a muffle furnace to obtain C–N–S-tridoped TiO₂. TiO₂ was also prepared as the method mentioned above without the presence of ammonium thiocyanate. The corresponding samples were labeled as 0% (TiO₂), 2%, 4%, 6%, 8% and 10%, respectively.

The specific surface area measurements were performed on a Quadrasorb automatic surface analyzer. X-ray diffraction (XRD) patterns were recorded on a DX-2600 X-ray diffractometer using Cu K α ($\lambda = 0.15406$ nm) radiation and equipped with a graphite monochromator. The X-ray tube was operated at 40 kV and 25 mA. The UV–Vis diffuse reflectance spectroscopy (DRS) was recorded using a TU-1901 UV–Vis spectrophotometer. Scanning electron microscope (SEM) images were taken with a JSM-7500F SEM, using an accelerating voltage of 5 kV. X-ray photoelectron spectroscopy (XPS) measurements were performed on an XSAM 800 using Mg K α at 12 kV and 12 mA. The X-ray photoelectron spectra were referenced to the C 1s peak (Binding energy (BE) = 284.80 eV) resulting from adventitious hydrocarbon (i.e., from the XPS instrument itself) present on the sample surface, and the measurement error is ± 0.1 eV. The measurements of surface photovoltage spectroscopy (SPS) were carried out on a home-built apparatus.

Photocatalytic activity experiments of MO were carried out in an SGY-II photochemical reactor (Kaifeng HXSCI Science Instrument Factory, China) as described in reference [7]. The illumination source was a 500 W high-pressure mercury lamp with a maximum emitting radiation of 365 nm. The concentration of MO aqueous solution was 10 mg/L, the dosage of photocatalyst was 1 g/L, the volume of MO was 50 mL, and the initial pH value of MO solution was 7.0 adjusted by HClO₄ and sodium hydroxide solution. The concentration of MO was analyzed at 460 nm through a spectrophotometer using Lambert–Beer law. Photocatalytic activity experiments of phenol were carried out in a Phchem III photochemical reactor (Beijing NBET Technology Co., Ltd., China) followed the procedures as described in reference [8]. The illumination source was a 500 W Xe lamp (simulated solar light). The dosage of photocatalyst was 1 g/L, the concentration of phenol aqueous solution was 10 mg/L, the volume of phenol was 50 mL and the initial pH value of phenol aqueous solution was 6.0. The concentration of phenol was measured by HPLC using an Agilent Technologies 1200 chromatograph equipped with UV–Vis detector operated at 270 nm and C18 column (5 μ m, 4.6 mm \times 150 mm). The HPLC analysis was carried out using water/methanol (60:40) as mobile phase with the flow rate of 0.8 mL/min. The chemical oxygen demand (COD) of MO and phenol solution was measured by a representative chemistry method (K₂Cr₂O₇–Ag₂SO₄). The removal of COD (γ) was calculated according to the following formula:

$$\gamma = \frac{\text{COD}_0 - \text{COD}_r}{\text{COD}_0} \times 100\%$$

where COD₀ and COD_r stand for the COD of MO/phenol solution before and after illumination, respectively. All reported data were the average values of three parallel determinations.

3. Results and discussion

3.1. Characterization of photocatalysts

The XRD patterns of the photocatalysts are shown in Fig. 1. For the bare TiO₂, peaks of anatase and rutile are simultaneously observed. However, the peaks of rutile gradually decrease as the amount of C–N–S increases, for 6%, 8% and 10% samples, all the strong peaks can be indexed as the pure anatase-type TiO₂, which fits well with the reported data (JCPDS 71-1169). This observation substantially illustrates that C–N–S can effectively retard the anatase–rutile transition of TiO₂, which is in good agreement with the results reported by Zhang et al. [9]. Moreover, the average crystallite size of (101) peak can be estimated using the Scherrer equation. The results show that the average crystallite size of 0%, 2%, 4%, 6%, 8% and 10% samples are 3.2, 2.6, 2.0, 1.9, 1.8 and 1.5 nm, respectively. The results suggest that C–N–S doped inhibits the growth of crystal; the reason is that the crystal structure of titania was affected by the incorporation of the dopants. This result accords well with the result of Brunauer–Emmett–Teller. The specific surface area of 0%, 2%, 4%, 6%, 8% and 10% is 7.6, 9.3, 11.4, 11.3, 10.8 and 13.7 m²/g, respectively. High specific surface area of the photocatalyst can provide more surface active sites, thus the reactive species have more chance to react with the adsorbed organic pollutants, promoting the photocatalytic activity.

Due to the partial overlap of UV–Vis DRS of photocatalysts, thus only the DRS of TiO₂, 2%, 6% and 8% samples are presented in Fig. 2. Compared with the bare TiO₂, the DRS of 2%, 6% and 8% samples appear blueshift, which demonstrates that C–N–S codoping widens the band gap. The results here are different from the results reported by Wang et al. [10]. The difference may ascribe to the different dopant source and after treatment temperature, and more detailed mechanism needs to be further investigated in the

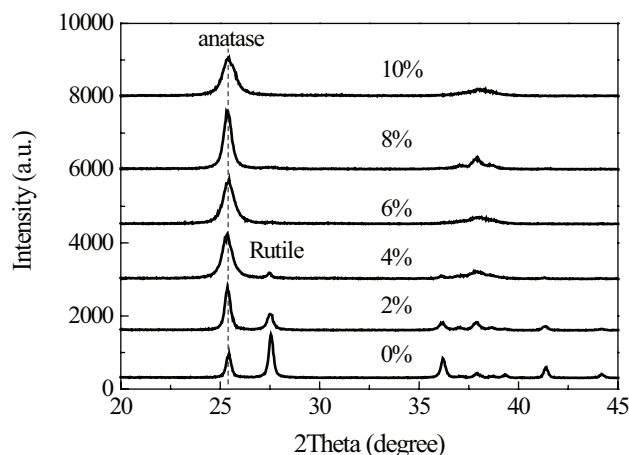


Fig. 1. XRD patterns of photocatalysts.

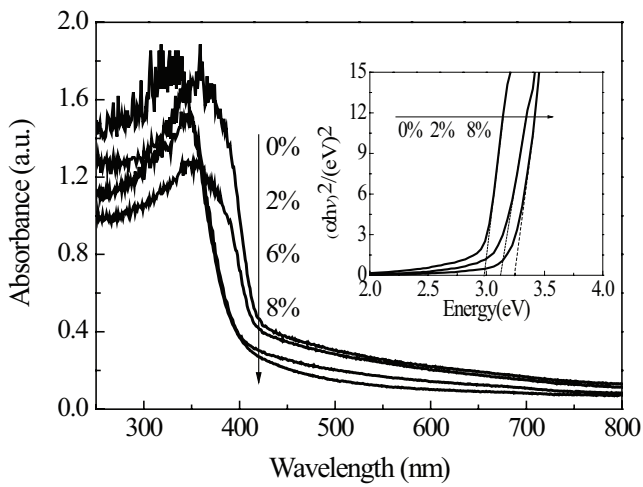


Fig. 2. UV/Vis DRS of photocatalysts.

near future. The band gap of 0%, 2% and 8% samples is presented in Fig. 2 (inset). The band gap is 2.98, 3.13 and 3.24 eV for 0%, 2% and 8% samples, respectively, indicating that C–N–S codoping widens the band gap of TiO_2 . Compared with the bare TiO_2 , the doped TiO_2 displays wide band gap, suggesting that valence band/conduction band of doped TiO_2 sample is more positive/negative than that of the reference TiO_2 , thus the photoinduced holes and electrons from the doped TiO_2 exhibit stronger oxidation/reduction ability than that of the bare TiO_2 , which is beneficial to photocatalytic performance.

The SEM images of TiO_2 , 2%, 6%, 8% and 10% samples are shown in Fig. 3. As shown in Fig. 3, 0% and 2% samples have irregular lump-like morphology. However, for the 6%, 8% and 10% samples, they have encephalon-like shape, thus it is reasonable to conclude that doping appropriate amount of C–N–S into TiO_2 can appreciably alter the morphology of TiO_2 .

The XPS spectra of 8% sample are displayed in Fig. 4. Three constituents situated at 288.6, 285.9 and 284.6 eV were

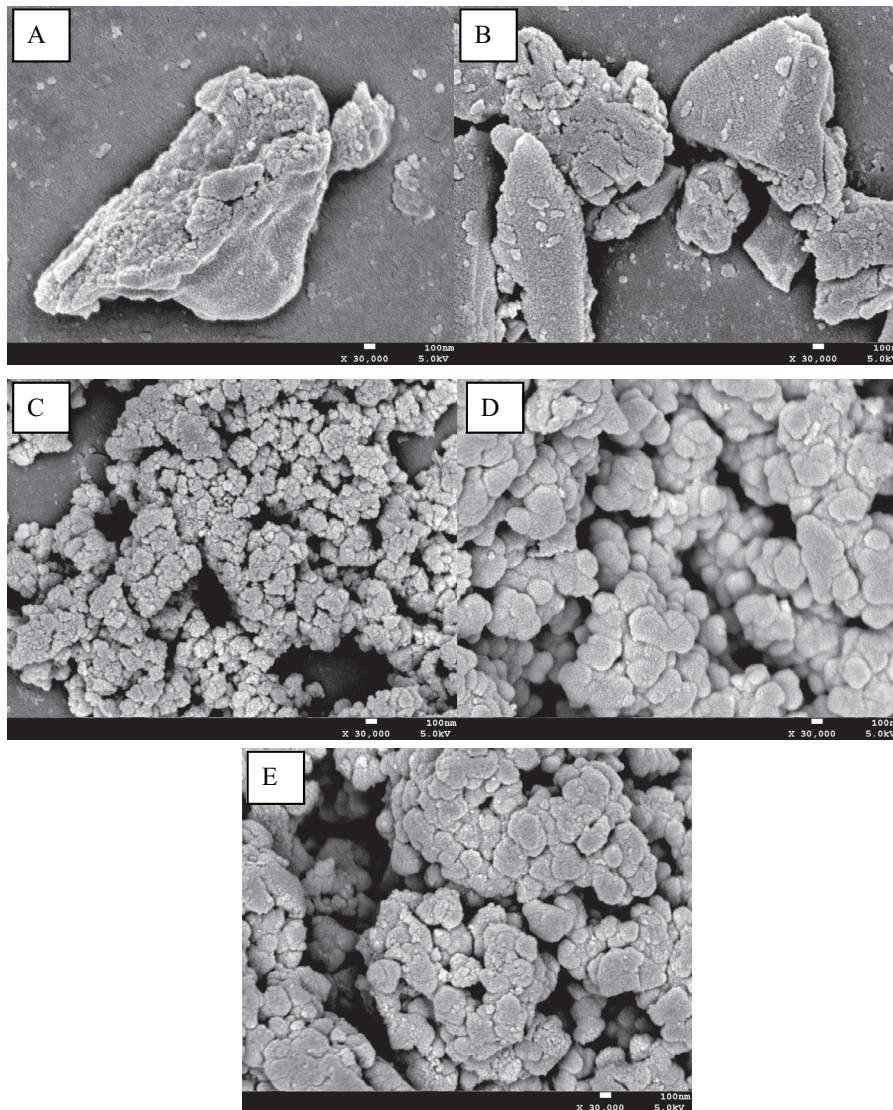


Fig. 3. SEM of photocatalysts: (A) 0%; (B) 2%; (C) 6%; (D) 8% and (E) 10%.

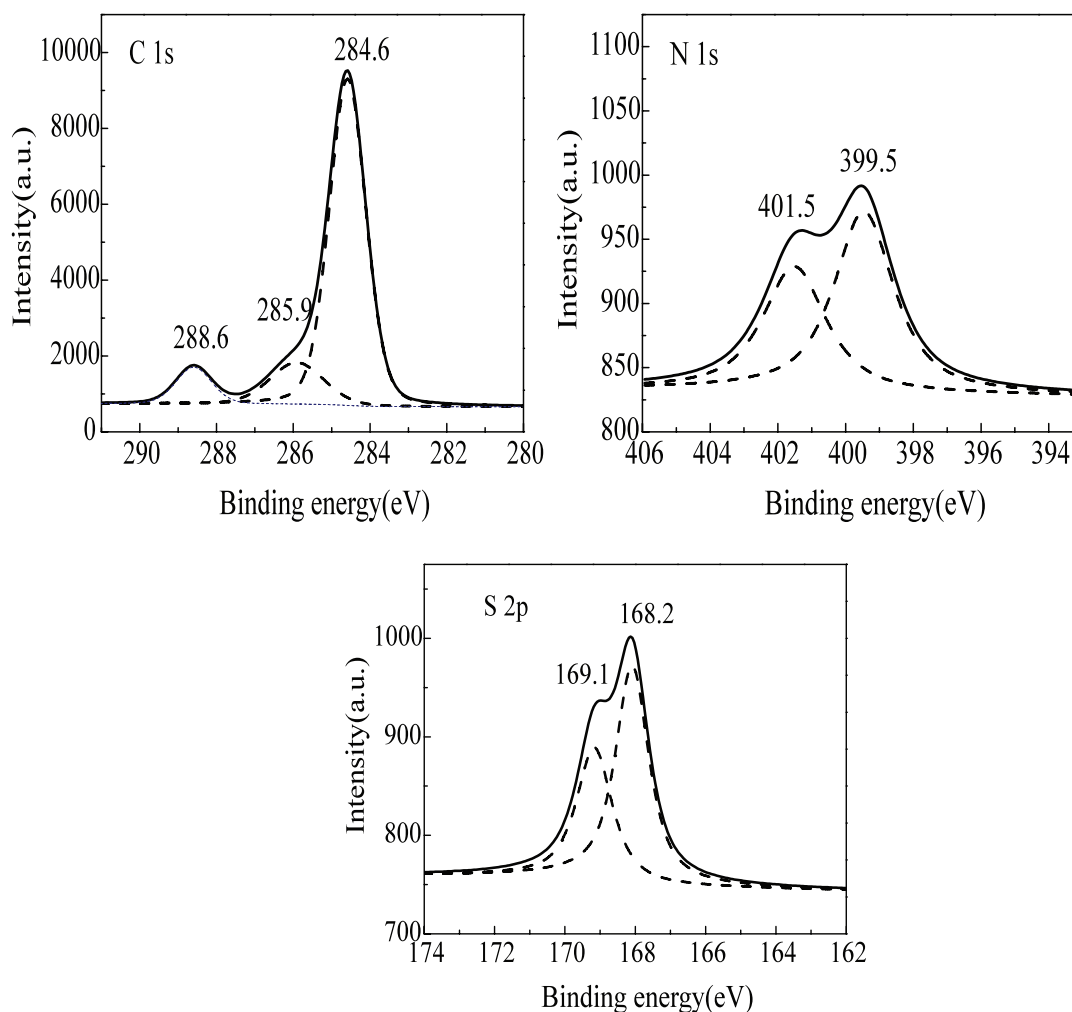


Fig. 4. XPS spectra of 8% sample.

observed for C 1s XPS spectra. The peaks located at 288.6 and 285.9 eV are assigned to C–O–Ti and C=O bonds, respectively [11,12]. The peak at 284.6 eV is adventitious carbon or residual carbon from the organic precursor. The peak of N 1s for the 8% sample can be fitted into two peaks, locating at 399.5 and 401.5 eV, which corresponds to the N 1s_{1/2} and N 1s_{3/2} [13], respectively. The peak at 399.5 eV is assigned to O–Ti–N, indicating that the substitution of some lattice oxygen sites by nitrogen [14,15]. The peak at 401.5 eV is assigned to interstitial nitrogen atoms [16]. The peaks at 168.2 and 169.1 eV can be attributed to S⁶⁺ in the lattice replace for Ti⁴⁺ [9], suggesting that the S was doped into the lattice of TiO₂. The results of XPS firmly confirm that C, N and S have been simultaneously doped into the lattice of TiO₂ using ammonium thiocyanate as dopant. As can be seen from Fig. 5, two oxygen signals located at 529 and 531 eV were detected, which are assigned to Ti–O and Ti–OH, respectively. The O 1s XPS spectrum can be further fitted into two kinds of chemical states by the Origin software with Gaussian–Lorentzian rule and the corresponding XPS data were listed in Table 1, where r_i (%) represents the ratio of the different kinds of oxygen contributions. Obviously, the content of hydroxyl oxygen on the

C–N–S doped TiO₂ is higher than that on the bare TiO₂, indicating that C–N–S tridoping increase the surface hydroxyl groups. Usually, the increment of surface hydroxyl content on the surface of TiO₂ is beneficial to the improvement of photocatalytic performance. Fig. 6 shows the high-resolution XPS spectra of the Ti 2p_{3/2} region taken on the surface of TiO₂ and C–N–S doped TiO₂. Compared with the pure TiO₂, Ti 2p binding energies of C–N–S doped TiO₂ gradually shift to higher value as C, N and S content increasing. The shift of the Ti 2p value demonstrates that the electron density and chemical environments of Ti element have been changed by carbon, nitrogen and sulfur atoms [17].

The SPS of the bare TiO₂ and C–N–S doped TiO₂ samples is shown in Fig. 7. As shown in Fig. 7, the intensity of SPS increases gradually as the amount of ammonium thiocyanate increases; however, when the molar ratio of ammonium thiocyanate/Ti is 10%, the SPS response drops. It is plausible that excessive C, S and N doped result in more defects and become the recombination centers of photoinduced electron–hole pairs, resulting in a weaker SPS response. In general, strong SPS response corresponds to high separation rate of photoinduced charge pairs on the basis of the SPS

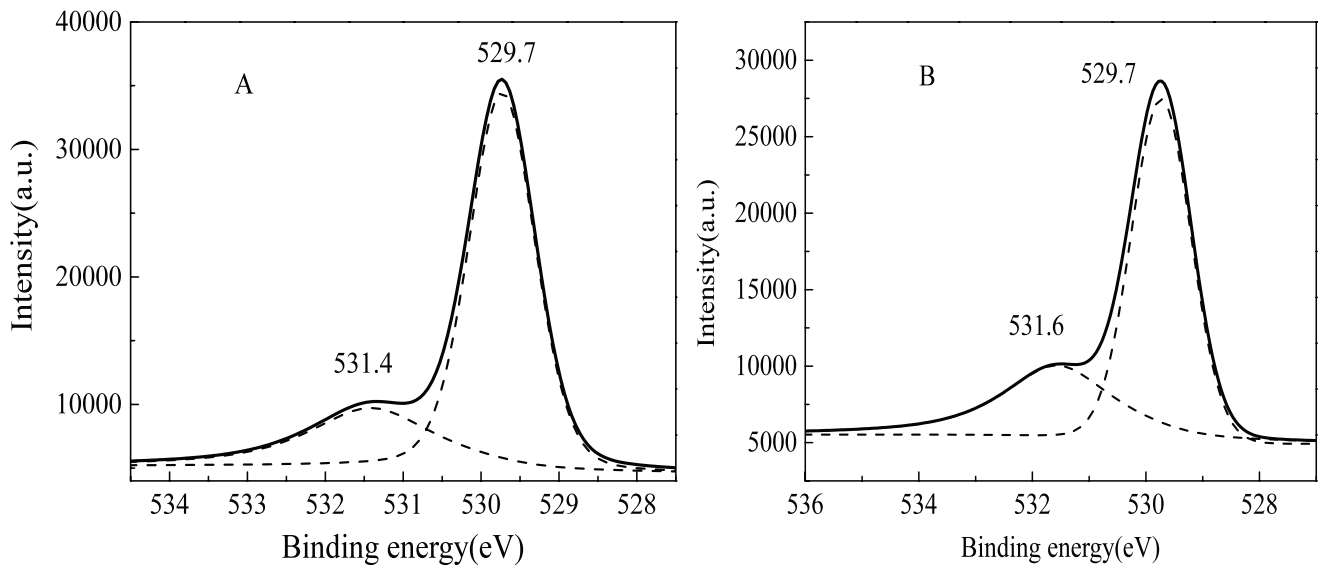


Fig. 5. High-resolution XPS spectra of the O 1s region on the surfaces of photocatalysts: (A) 0% and (B) 8%.

Table 1
Elemental surface compositions of as-synthesized photocatalysts by XPS

Photocatalyst	O 1s (Ti–O)		O 1s (O–H)	
	E_b (eV)	r_i (%)	E_b (eV)	r_i (%)
0%	529.7	73.4	531.4	26.6
8%	529.7	69.9	531.6	30.1

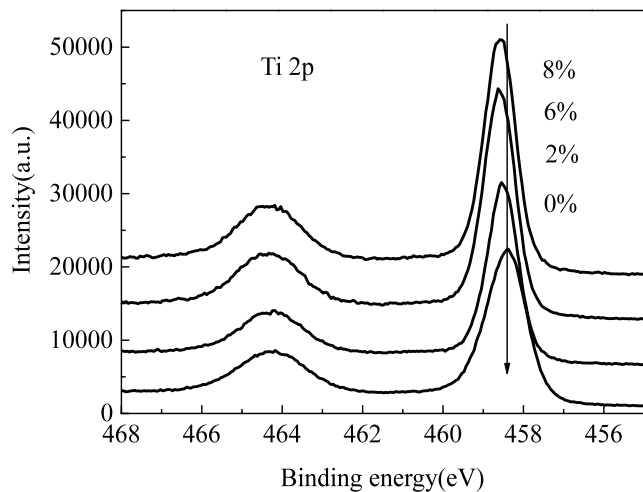


Fig. 6. XPS spectra of Ti 2p on photocatalysts.

principle [18,19]. The high charge separation rate is beneficial to the photocatalytic activity. Moreover, in the visible light region, no SPS was detected for the 0%, 2%, 4% and 6% samples. While for the 8% and 10% samples, weak SPS was observed, which may be due to the trapping states. The results of SPS fit well with the results of DRS and photocatalytic activity.

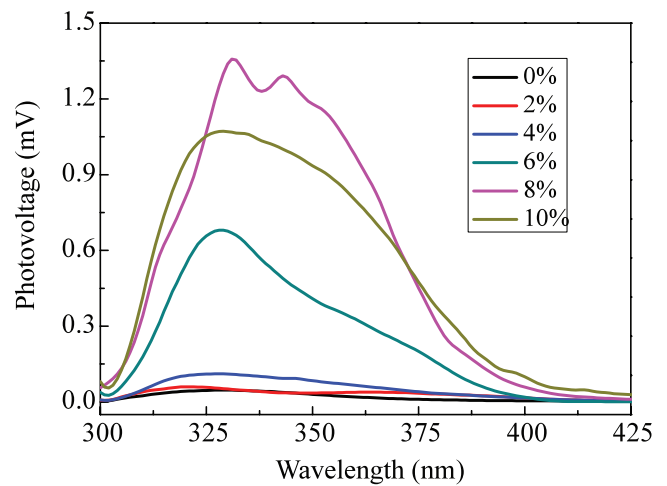


Fig. 7. SPS response of photocatalysts.

3.2. Photocatalytic activity

The photolysis of MO and phenol aqueous solution (10 mg/L) under irradiation without photocatalyst after 30 min is so small that can be totally ignored, and the adsorption of MO and phenol on different photocatalysts after 30 min in a dark is small than 5%. The photocatalytic activities of the bare TiO₂ and doped TiO₂ are shown in Fig. 8. As shown in Fig. 8, all C, N and S doped photocatalysts exhibit better photocatalytic activity than TiO₂ and the 8% sample displays the best photocatalytic activity among the experimented compositions. The degradation efficiency of MO and phenol over 8% is higher (52.5% and 13.5%) than that of the reference TiO₂. However, the catalytic activity of 10% sample is lower than that of 8%, excessive C, S and N result in more defects and become the recombination centers of photoinduced electron–hole pairs. Furthermore, as shown in Fig. 9, the removal of COD of MO and phenol increases as the ammonium thiocyanate content

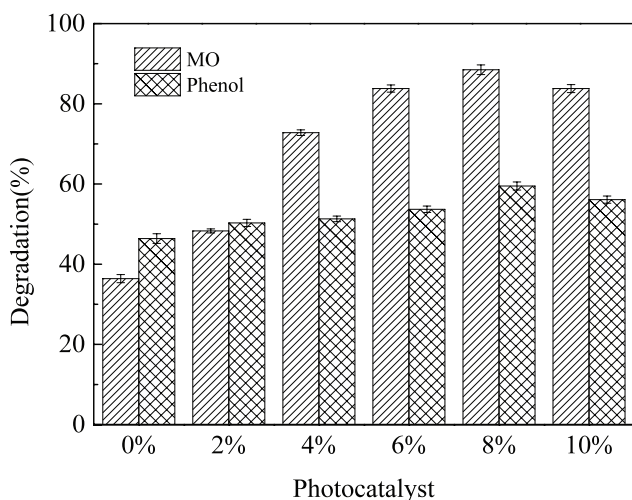


Fig. 8. Removal of methyl orange and phenol photolyzed over photocatalysts for 30 min.

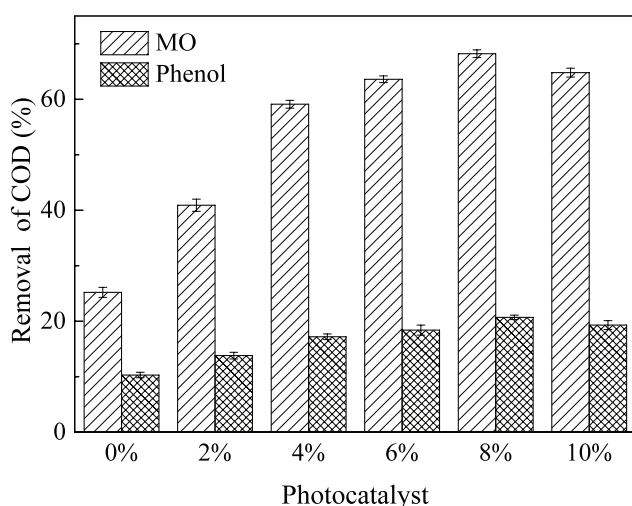


Fig. 9. COD removal of methyl orange and phenol over photocatalysts photolyzed for 30 min.

increasing, and reaches the highest when the ammonium thiocyanate content (ammonium thiocyanate/Ti) is 8%. In addition, degradation MO is faster and deeper than phenol, which may be due to the different light resource and stability of molecular structure. These results substantially demonstrate that photocatalytic activity of TiO_2 can be greatly enhanced by C–N–S tridoping. In this paper, the improved photocatalytic activity of C–N–S tridoped TiO_2 may attribute to the increased specific surface area of photocatalysts, strong redox ability of photon-generated electrons and holes, and high surface hydroxyl content and promoted separation rate of photoinduced charge carriers.

4. Conclusions

C–N–S-tridoped TiO_2 photocatalysts were successfully prepared by a facile sol–gel routine using ammonium thiocyanate as dopant. Doping of TiO_2 by C, N and S inhibits

the growth of the crystal and the anatase–rutile transition, widens the band gap, changes the shape of particle and the surface hydroxyl content, and enhances the photoinduced charge separation rate. When the molar ratio of ammonium thiocyanate/ TiO_2 is 8%, the sample exhibits the best photocatalytic activity towards degradation of MO and phenol. Doping C, N and S into TiO_2 using ammonium thiocyanate as dopant is a simple and effective way to enhance the photocatalytic performance of TiO_2 .

Acknowledgments

This project was supported financially by the Opening Project of Key Laboratory of Green Catalysis of Sichuan Institutes of High Education (No. LZJ1301, No. LYJ14203), Construct Program of the Discipline in Sichuan University of Science and Engineering and Sichuan Provincial Academician (Expert) Workstation (No. 2015YSGZZ03).

References

- [1] S.T. Wei, X.L. Hu, H.L. Liu, Q. Wang, C.Y. He, Rapid degradation of Congo red by molecularly imprinted polypyrrole-coated magnetic TiO_2 nanoparticles in dark at ambient conditions, *J. Hazard. Mater.*, 294 (2015) 168–176.
- [2] J.Q. Qi, X.C. Li, H. Zheng, P.Q. Li, H.Y. Wang, Simultaneous removal of methylene blue and copper(II) ions by photoelectron catalytic oxidation using stannic oxide modified iron(III) oxide composite electrodes, *J. Hazard. Mater.*, 293 (2015) 105–111.
- [3] A.L. Linsebigler, G. Lu, J.T. Yates Jr., Photocatalysis on TiO_2 surfaces: principles, mechanisms, and selected results, *Chem. Rev.*, 95 (1995) 735–758.
- [4] M.R. Hoffmann, S.T. Martin, W. Choi, D.W. Bahnemann, Environmental applications of semiconductor photocatalysis, *Chem. Rev.*, 95 (1995) 69–96.
- [5] X.F. Lei, X.X. Xue, H. Yang, C. Chen, X. Li, M.C. Niu, X.Y. Gao, Y.T. Yang, Effect of calcination temperature on the structure and visible-light photocatalytic activities of (N, S and C) co-doped TiO_2 nano-materials, *Appl. Surf. Sci.*, 332 (2015) 172–180.
- [6] J.G. Yu, X.J. Zhao, Q.N. Zhao, J.C. Du, XPS of study of TiO_2 photocatalytic thin film prepared by the sol-gel method, *Chin. J. Mater. Res.*, 14 (2000) 203–209.
- [7] Z.H. Xiao, J.B. Zhong, J.Z. Li, S.T. Huang, J. Zeng, M.J. Li, G. Yong, Enhanced photocatalytic activity of Y and Pd-co-doped Bi_2O_3 prepared by parallel flow co-precipitation method, *J. Adv. Oxid. Technol.*, 17 (2014) 139–144.
- [8] J.B. Zhong, J.Z. Li, X.L. Liu, Q.Z. Wang, H. Yang, W. Hu, C.Z. Cheng, J.B. Song, M.J. Li, T. Jin, Enhanced photo-induced charge separation and solar-driven photocatalytic activity of g- C_3N_4 decorated by SO_4^{2-} , *Mater. Sci. Semicond. Process.*, 40 (2015) 508–515.
- [9] G.S. Zhang, Y.C. Zhang, M. Nadagouda, C. Han, K. O’Shea, S.M. El-Sheikh, A.A. Ismail, D.D. Dionysiou, Visible light-sensitized S, N and C co-doped polymorphic TiO_2 for photocatalytic destruction of microcystin-LR, *Appl. Catal., B*, 144 (2014) 614–621.
- [10] P.H. Wang, P.S. Yap, T.T. Lim, C-N-S tridoped TiO_2 for photocatalytic degradation of tetracycline under visible-light irradiation, *Appl. Catal., A*, 399 (2011) 252–261.
- [11] Y.D. Hou, X.C. Wang, L. Wu, Z.X. Ding, X.Z. Fu, Efficient decomposition of benzene over a beta- Ga_2O_3 photocatalyst under ambient conditions, *Environ. Sci. Technol.*, 40 (2006) 5799–5803.
- [12] Y. Zhang, Z. Zhao, J. Chen, L. Cheng, J. Chang, W. Sheng, C. Hu, S. Cao, C-doped hollow TiO_2 spheres: in situ synthesis, controlled shell thickness, and superior visible-light photocatalytic activity, *Appl. Catal., B*, 165 (2015) 715–722.
- [13] N.T. Nolana, D.W. Synnott, M.K. Seery, S.J. Hinder, A.V. Wassenhoven, S.C. Pillai, Effect of N-doping on the

- photocatalytic activity of sol-gel TiO₂, *J. Hazard. Mater.*, 211–212 (2012) 88–94.
- [14] R. Asahi, T. Morikawa, T. Ohwaki, K. Aoki, Y. Taga, Visible-light photocatalysis in nitrogen-doped titanium oxides, *Science*, 293 (2001) 269–271.
- [15] Y. Cong, J.L. Zhang, F. Chen, M. Anpo, Synthesis and characterization of nitrogen-doped TiO₂ nanophotocatalyst with high visible light activity, *J. Phys. Chem. C*, 111 (2007) 6976–6982.
- [16] T. Sano, N. Negishi, K. Koike, K. Takeuchi, S. Matsuzawa, Preparation of a visible light-responsive photocatalyst from a complex of Ti⁴⁺ with a nitrogen containing ligand, *J. Mater. Chem.*, 14 (2004) 380–384.
- [17] X. Cheng, X. Yu, Z. Xing, One-step synthesis of visible active C-N-S-tridoped TiO₂ photocatalyst from biomolecule cysteine, *Appl. Surf. Sci.*, 258 (2012) 7644–7650.
- [18] L.Q. Jing, J. Wang, Y. Qu, Y. Luan, Effects of surface-modification with Bi₂O₃ on the thermal stability and photoinduced charge property of nanocrystalline anatase TiO₂ and its enhanced photocatalytic activity, *Appl. Surf. Sci.*, 256 (2009) 657–663.
- [19] L. Mohapatra, K. Parida, M. Satpathy, Molybdate/tungstate intercalated oxo-bridged Zn/Y LDH for solar light induced photodegradation of organic pollutants, *J. Phys. Chem. C*, 116 (2012) 13063–13070.